ARTICLE IN PRESS

Available online at www.sciencedirect.com
SCIENCE DIRECT®

Atmospheric Environment ▮ (▮▮▮▮) ▮▮▮–▮▮▮

ATMOSPHERIC ENVIRONMENT

www.elsevier.com/locate/atmosenv

A PDF micromixing model of dispersion for atmospheric flow. Part I: development of the model, application to homogeneous turbulence and to neutral boundary layer

M. Cassiani[a,*], P. Franzese[b], U. Giostra[a]

[a]*Facoltà di Scienze Ambientali, Università di Urbino, Campus Scientifico Sogesta, 61029 Urbino, Italy*
[b]*School of Computational Sciences, George Mason University, Fairfax, Virginia 22030, USA*

Received 5 April 2004; received in revised form 5 November 2004; accepted 17 November 2004

Abstract

A Lagrangian stochastic (LS) probability density function (PDF) model has been developed to study statistics and PDF of concentration generated by continuous releases of passive substances from point and line sources in atmospheric flow. The model simulates the combined effect of turbulent mixing (macromixing) and molecular diffusivity (micromixing) on dispersion of tracers. Turbulent dispersion is modelled using an LS model; molecular diffusivity is simulated by an interaction by exchange with the conditional mean (IECM) model. A dynamical computational grid, which expands with time around the plume, has been developed to optimise computational time and memory requirements. The model has been tested with the results of a two-particle LS model in homogeneous turbulence and with wind tunnel observations in a neutral boundary layer. The proposed model can account for chemical reactions in a direct way with no closure assumptions.

Keywords: Concentration fluctuations; Micromixing modelling; Monte Carlo simulation; Turbulent dispersion; Chemical reactions

1. Introduction

Much research has been devoted to model the mean concentration field of substances released in the atmospheric boundary layer and modelling systems for mean concentration are routinely applied in air quality monitoring activities. Nevertheless, applications such as study of toxic gas effects on humans (e.g., Griffith and Megson, 1984; Hilderman et al., 1999), flammability of substances (e.g., Wilson, 1995), and interaction between turbulence and chemistry (e.g., Fox, 2003) require estimates of second and higher order moments of concentration, or even the full one-time one-point probability density function (PDF) of concentration.

LS fluctuating plume models (Luhar et al., 2000; Cassiani and Giostra, 2002; Franzese, 2003) are valuable tools for the estimation of all moments of concentration of non-reactive scalars in the convective boundary layer (CBL), and can be easily adapted to simulations in a neutral boundary layer. These models use parameterised in-plume relative concentration fluctuations because a closed theory is not available, but experimental measurements are scarce and case specific.

Georgopoulis and Seinfeld (1986) survey on reactive plume models includes the PDF formulations of O'Brien et al. (1976) and Dopazo (1976) "for completeness", as

*Corresponding author. Tel.: +39 722 304249; fax: +39 722 304265.
E-mail address: massimo.cassiani@uniurb.it (M. Cassiani).

1352-2310/$ - see front matter © 2004 Elsevier Ltd. All rights reserved.
doi:10.1016/j.atmosenv.2004.11.020

they stated, because their applications in the atmosphere required too intensive computational resources. Since then, these models and the available computer power have been greatly enhanced.

In a PDF formulation, the following equation for the one-point one-time joint PDF for velocity and scalar is derived from the Navier–Stokes equations (Pope, 1985):

$$\frac{\partial f_{c\mathbf{u}}}{\partial t} + v_i \frac{\partial f_{c\mathbf{u}}}{\partial x_i} + \frac{\partial}{\partial \varsigma}\left[f_{c\mathbf{u}} S(\varsigma)\right] = -\frac{\partial}{\partial v_i}\left(f_{c\mathbf{u}}\left\langle \nu\nabla^2 u_i - \frac{1}{\rho}\frac{\partial p}{\partial x_i}\middle| \mathbf{u}=\mathbf{v}, c=\varsigma\right\rangle\right) - \frac{\partial}{\partial \varsigma}(f_{c\mathbf{u}}\langle \Gamma\nabla^2 c|\mathbf{u}=\mathbf{v}, c=\varsigma\rangle), \quad (1)$$

where angle brackets denote ensemble average, ν is the viscosity of the fluid, Γ is the molecular diffusivity of the scalar, ς is the sample space variable for scalar concentration c (if multiple scalars are involved c_α represents the composition vector), $\mathbf{v}$ is the sample space variable for the velocity vector $\mathbf{u}$, and $f_{c\mathbf{u}} = f(\mathbf{v}, \varsigma; x, t)$ is the Eulerian joint PDF of velocity and concentration.

The third term on the left hand side is the chemical source, which appears in closed form—Eq. (1) is typically applied to problems of turbulent combustion mainly because of its property of including chemical reactions without closure approximations (see e.g., Pope, 1985; Dopazo et al., 1997). On the right-hand side, the first term represents the effect of viscous stresses and pressure gradient and the last term is associated with the transport in composition space by molecular fluxes.

Pope (1994, 2000) and Heinz (2003) reviewed various closures and modelling techniques for the viscous stresses and pressure gradient terms in the form of Lagrangian stochastic differential equations for velocity and position of the fluid particles. In the one-particle stochastic theory the one-point one-time PDF of velocity is assumed to be known. The equations for velocity and position are usually solved only for marked particles released from the source, but they describe as well the motion of all particles in the flow, according to the well-mixed condition (Thomson, 1987).

The term associated with molecular diffusivity in Eq. (1) defines the shape of the PDF of concentration, and its closure is usually referred to as the micromixing model. A micromixing model describes the evolution of the PDF of concentration using an additional equation for the concentration carried by each particle in the domain. Therefore, a PDF model includes a set of equations for velocity, position and concentration of each fluid particle. This separation of the effects of turbulent mixing and molecular processes is typical of a variety of modelling approaches (see, e.g., the short review by Kernstein, 1991).

Various micromixing models have been proposed so far (see the review by Dopazo et al., 1997). Fox (2003) reports a set of constraints and desirable properties deduced from the conservation equations, DNS data and experiments. Summarizing we can restate these constraints as: (i) at high Reynolds number the mean scalar fields must not be affected by micromixing; (ii) micromixing must dissipate the fluctuations; (iii) the scalar field must be bounded. A desirable property that is often invoked is: (iv) for homogeneous turbulent mixing (i.e., statistically homogeneous scalar fields in homogeneous isotropic turbulence) the scalar PDF should tend to a normal. Property (iv) is somewhat in contrast with constraint (iii). Also, Chatwin (2004) argued that the PDF should tend asymptotically to a Dirac delta function about the mean, $\delta(\varsigma - \langle c\rangle)$, where $\langle c\rangle$ tends to a positive value (mass/volume) in bounded volumes and to zero in unbounded domains. However, in general it is assumed that the Gaussian can be taken as a reasonable approximation of the theoretical asymptotic PDF.

The simplest and most common micromixing model in turbulent combustion applications is the IEM model (Interaction by Exchange with the Mean, Villermaux and Devillon, 1972), also called LMSE model (Linear Mean Square Estimation, Dopazo and O'Brien, 1974). It is based on a linear relaxation of the local concentration towards the local mean,

$$\langle \Gamma\nabla^2 c|\mathbf{u}=\mathbf{v}, c=\varsigma\rangle = -\frac{1}{t_m}(\varsigma - \langle c\rangle) \quad (2)$$

with a characteristic time of relaxation t_m, also called micromixing time scale. The model reflects the concept that the ultimate action of mixing is to homogenise the concentration field, thus dissipating the fluctuations. The relaxation towards the mean mimics this dissipative behaviour. It can be shown that the above equation is exact in the case of homogeneous turbulent mixing of initially Gaussian scalar PDF (see e.g., Pope, 2000).

This model has been applied to atmospheric turbulence by Gonzalez (1997) using a Markov assumption on the particle position (the traditional k-closure). In Bisignanesi et al. (2002) the IEM model has been coupled with a Thomson (1987) model for velocity and position to simulate the laboratory experiments of diffusion of reactive scalars (Li and Bilger, 1996). The IEM model has the merit of simplicity but also two major shortcomings. The first is the inability to fulfil property (iv); in fact this model preserves the shape of the PDF for a statistically homogeneous scalar field (Pope, 2000). The importance of this shortcoming depends on the application: for instance, property (iv) is not a necessary condition for satisfactory performance in inhomogeneous flows (Subramaniam and Pope, 1998). The model correctly predicts the

asymptotic Gaussian for homogeneous turbulent mixing with a constant mean scalar gradient and, in general, the correct asymptotic behaviour can be reached in the presence of strong mean scalar inhomogeneities. The second shortcoming is the inability to fulfil constraint (i) due to the creation of spurious fluxes, which alter the mean concentration field, as shown by Pope (1998) and further investigated by Sawford (2004).

In order to solve the problem of spurious fluxes, a modified IEM model, called IECM (Interaction by Exchange with the Conditional Mean) was developed (Fox, 1996; Pope, 1998). In this model, the concentration relaxes to the mean concentration conditioned over the velocity

$$\langle \Gamma \nabla^2 c | \mathbf{u} = \mathbf{v}, c = \varsigma \rangle = -\frac{1}{t_m}(\varsigma - \langle c | \mathbf{u} = \mathbf{v} \rangle). \tag{3}$$

In general, the relaxation towards a conditional mean allows to better respect the principle of localness (see Pope, 1998; Subramaniam and Pope, 1998), i.e., particles that interact with each other have similar position, velocity and concentration. Conceptually, one can think of velocity-conditioned scalar mixing as occurring between fluid elements that belong to the same physical eddy (Fox, 1996). Sawford (2004) provided insight of the physical foundations of this technique showing that it can be related to a meandering plume model, and successfully applied it to the dispersion of a passive scalar released from a line source in grid-generated turbulence. Luhar and Sawford (2005) used the IECM approach to model concentration fluctuations in a convective boundary layer. The IECM, like the IEM model, fails to fulfil property (iv); in fact the two models are equivalent in conditions of homogeneous turbulent mixing since the velocity and the scalar are uncorrelated (Fox, 1996).

In this paper, the IECM technique is used to develop a model for the PDF of concentration of passive scalars. The model is applied to releases in homogeneous turbulence and in the atmospheric neutral boundary layer. The complete set of model equations is introduced in Section 2; a simple semi-empirical model for the micro mixing time scale is described in Section 3. An efficient algorithm based on a dynamical time-expandable grid is developed and is described in Section 4. In Section 5, simulated concentration statistics and PDF are compared with the results of Thomson's (1990) two-particle Lagrangian stochastic model for homogeneous turbulence, and with Fackrell and Robins (1982a) wind tunnel observations in a neutral boundary layer.

In the following, we will not use the distinction between random and sample space variable: we will simply refer to c as concentration and $\mathbf{u}$ as velocity.

2. Model equations

The following set of stochastic differential equations can be used to describe the evolution of velocity, position and concentration of a passive particle:

$$\mathrm{d}U_i = a_i(\mathbf{X}, \mathbf{U}, t)\mathrm{d}t + b_{ij}(\mathbf{X}, \mathbf{U}, t)\mathrm{d}\zeta_j, \tag{4}$$

$$\mathrm{d}X_i = U_i \mathrm{d}t, \tag{5}$$

$$\mathrm{d}C = \varphi(C, \mathbf{X}, \mathbf{U}, t)\mathrm{d}t + h(C, \mathbf{X}, \mathbf{U}, t)\mathrm{d}\zeta, \tag{6}$$

where the capital letters indicate particle (i.e., Lagrangian) quantities. $\mathbf{U}$ and $\mathbf{X}$ are the particle velocity and position vectors respectively, C is the concentration associated with the particle, $\mathrm{d}\zeta_j$ indicates a vector of independent Wiener processes with zero mean and variance $\mathrm{d}t$ (see Gardiner, 1983), and $\mathrm{d}\zeta$ indicates another independent Wiener process. The terms a_i and b_{ij} jointly model the term associated with viscous stresses and pressure gradient in Eq. (1), the term φ models the conditional scalar dissipation term. Because the scalar is passive, the velocity is independent of the concentration field. In the case of reactive scalar, chemical reactions can be included directly in the term φ. In the case of multiple scalars, C should be replaced by the concentration vector associated with the particle. The extension to multiple reactive scalars requires some additional assumptions (see Pope, 2000).

The above equations are based on a Markov assumption for velocity and concentration. The validity of a Markov assumption for velocity is discussed in Thomson (1987) or Monin and Yaglom (1975) and is usually accepted. The validity of a Markov assumption for concentration is less explored, although Wandel et al. (2003) show that its level of accuracy is comparable to the Markov assumption for velocity. The use of a stochastic differential equation for the particle concentration also provides for a continuous evolution and fulfils property (iv) (see Dopazo et al., 1997; Heinz, 2003). However, its implementation can be difficult because the concentration field is bounded, and the Wiener process should be substituted by a binomial process, or by a dichotomic process to simplify the computation (Dopazo et al., 1997).

We follow a simpler deterministic approach in the formulation of the evolution equation for the concentration of each particle, i.e.,

$$\mathrm{d}C = \varphi(C, \mathbf{X}, \mathbf{U}, t)\mathrm{d}t. \tag{7}$$

Eqs. (4), (5) and (7) correspond to the following Fokker–Plank equation for the evolution of the Eulerian joint PDF $f_{c\mathbf{u}}$

$$\frac{\partial f_{c\mathbf{u}}}{\partial t} = -\frac{\partial}{\partial x_i}(u_i f_{c\mathbf{u}}) - \frac{\partial}{\partial u_i}(a_i f_{c\mathbf{u}}) + \frac{\partial^2}{\partial u_i \partial u_j}(B_{ij} f_{c\mathbf{u}}) - \frac{\partial}{\partial c}(\varphi f_{c\mathbf{u}}) \tag{8}$$

with $B_{ij} = b_{ik}b_{jk}/2$. From the comparison with Eq. (1) it can be seen that the term φ models the effect of molecular diffusivity.

The coefficient φ is specified according to the IECM theory, i.e.,

$$\frac{\mathrm{d}C}{\mathrm{d}t} = -\frac{1}{t_\mathrm{m}}(C - \langle c|\mathbf{X},\mathbf{U}\rangle), \tag{9}$$

where $\langle c|\mathbf{X},\mathbf{U}\rangle$ is the ensemble mean concentration conditioned on the particle position and particle velocity vectors. The micromixing time scale t_m will be defined in the next section.

The coefficient $b_{ij}(\mathbf{X},\mathbf{U},t)$ is obtained imposing consistency with the Lagrangian structure function in the inertial sub range, i.e., $b_{ij} = \delta_{ij}(C_0\varepsilon)^{1/2}$, where C_0 is the Kolmogorov constant and ε is the mean dissipation of turbulent kinetic energy. The coefficient $a_i(\mathbf{X},\mathbf{U},t)$ is obtained ensuring the fulfilment of the well-mixed condition, namely the consistency of Eqs. (4) and (5) with the marginal PDF of the Eulerian velocity $f_\mathbf{u}(\mathbf{v};\mathbf{x},t)$ through the following Fokker–Planck equation (Thomson, 1987)

$$\frac{\partial f_\mathbf{u}}{\partial t} = -\frac{\partial}{\partial x_i}(u_i f_\mathbf{u}) - \frac{\partial}{\partial u_i}(a_i f_\mathbf{u}) + \frac{\partial^2}{\partial u_i \partial u_j}(B_{ij} f_\mathbf{u}), \tag{10}$$

which provides

$$a_i = \frac{1}{f_\mathbf{u}}\left[\frac{\partial}{\partial u_i}(B_{ij} f_\mathbf{u}) + \Phi_i(\mathbf{x},\mathbf{u},t)\right] \tag{11}$$

with

$$\frac{\partial \Phi_i}{\partial u_i} = -\frac{\partial f_\mathbf{u}}{\partial t} - \frac{\partial}{\partial x_i}(u_i f_\mathbf{u}). \tag{12}$$

Hereinafter, we will refer to turbulent velocities as the velocity field. Mean wind speed and direction ($i = 1$) are assumed to be known. The classical meteorological notation $(x, y, z) = (x_1, x_2, x_3)$ and $(u, v, w) = (u_1, u_2, u_3)$ will be used instead of the indicial notation where more convenient.

For emissions from a continuous point or line source the dispersion in the along wind direction can be neglected if $\sigma_u \ll \langle u\rangle$. We use this assumption to reduce the problem to two dimensions for point sources and to one dimension for crosswind line sources.

For neutral boundary layer we use the form $f_\mathbf{u} = g_{u_2} g_{u_3}$ for the two-dimensional PDF of velocity in the transverse directions, where g indicates a Gaussian

$$g_{u_i} = \frac{1}{\sqrt{2\pi}\sigma_{u_i}} \exp\left(-\frac{u_i^2}{2\sigma_{u_i}^2}\right), \tag{13}$$

where $\sigma_{u_i}^2 = \langle u_i^2\rangle$. Thus, Eq. (4) for the transverse velocity components can be written in explicit form:

$$\mathrm{d}V = \left[W\frac{\partial \sigma_v^2}{\partial z} - C_0\varepsilon\right]\frac{V}{2\sigma_v^2}\,\mathrm{d}t + (C_0\varepsilon)^{1/2}\mathrm{d}\zeta_2, \tag{14}$$

$$\mathrm{d}W = \frac{1}{2\sigma_w^2}\left[\frac{\partial \sigma_w^2}{\partial z}(\sigma_w^2 + W^2) - C_0\varepsilon W\right]\mathrm{d}t + (C_0\varepsilon)^{1/2}\mathrm{d}\zeta_3, \tag{15}$$

where all turbulence statistics are evaluated at particle position.

In homogeneous isotropic turbulence the above equations simplify to a standard Ornstein–Uhlenbeck process in both directions (Gardiner, 1983)

$$\mathrm{d}U_i = -\frac{C_0\varepsilon}{2\sigma_{ui}^2}\,U_i\,\mathrm{d}t + (C_0\varepsilon)^{1/2}\mathrm{d}\zeta_i. \tag{16}$$

3. The scalar micromixing time scale

In this section, we present a simple semi-empirical formulation for the micromixing time scale. The IECM conservation equation for the concentration variance, $\sigma_c^2 \equiv \langle c'^2\rangle = \langle (c - \langle c\rangle)^2\rangle$ can be obtained from Eq. (8) is written, in the absence of a mean velocity field, as

$$\frac{\partial\langle c'^2\rangle}{\mathrm{d}t} + \frac{\partial\langle uc'^2\rangle}{\partial x_i} + 2\langle u_i c'\rangle\frac{\partial\langle c\rangle}{\partial x_i} = -\frac{2}{t_\mathrm{m}}\left[\langle c'^2\rangle - \langle\langle c'|\mathbf{u}\rangle^2\rangle_\mathbf{u}\right], \tag{17}$$

which shows that t_m is related to the square of a conditional mean. In condition of homogeneous turbulent mixing with no mean scalar gradient $\langle c'|\mathbf{u}\rangle \to 0$ because the velocity and scalar fields are uncorrelated (Fox, 1996). In this case, Eq. (17) is the same as for IEM model.

The scalar dissipation rate, $\varepsilon_\mathrm{c} \equiv 2\Gamma\langle\partial c/x_i\,\partial c/x_i\rangle$, can be determined comparing Eq. (17) with the standard Reynolds averaged equation for the concentration variance, we can see that at high Reynolds number: $\varepsilon_\mathrm{c} = 2/t_\mathrm{m}[\langle c'^2\rangle - \langle\langle c'|\mathbf{u}\rangle^2\rangle_\mathbf{u}]$. From Eq. (17) and the definition of the dissipation time scale of concentration variance $\tau_\mathrm{c} \equiv 2\sigma_\mathrm{c}^2/\varepsilon_\mathrm{c}$ we obtain the following relation:

$$t_\mathrm{m} = \tau_\mathrm{c}\left[1 - \langle\langle c'|\mathbf{u}\rangle^2\rangle_\mathbf{u}/\sigma_\mathrm{c}^2\right]. \tag{18}$$

The above relationship shows that for the IEM model $t_\mathrm{m} = \tau_\mathrm{c}$, while for the IECM model $t_\mathrm{m} = \tau_\mathrm{c}$ only in conditions of homogeneous turbulent mixing with no mean scalar gradient. Also, under these conditions $\tau_\mathrm{c} \approx \tau \equiv k/\varepsilon$, where k is the turbulent kinetic energy. τ_c is usually modelled according to this equilibrium relation within a k–ε modelling framework. Similarly, t_m is often modelled in PDF simulation using the IEM model. Although this assumption is exact only for homogeneous turbulent mixing, it is widely used and several DNS simulations and laboratory experiments

Table 1
Values of the ratio between turbulent and scalar dissipation time scale expressed as $2\tau/\tau_c = (k\varepsilon_c)/(\sigma_c^2\varepsilon)$

Authors	$2\tau/\tau_c$	Type of investigation	Notes
Eswaran and Pope (1988)	≈ 2	DNS of homogeneous turbulent mixing	
Overholt and Pope (1996)	1.8–3	DNS of homogeneous turbulent mixing with constant mean scalar gradient	Systematic Re dependence
Heinz (2003)	2.5	Theoretical extrapolation from DNS data of Overholt and Pope (1996)	$Re \to \infty$
Warhaft (2000)	1.5	Measurements in decaying grid turbulence with mean scalar gradient	
Tavoularis and Corrsin (1981)	2.17–3.12	Measurements in homogeneous sheared turbulence	
Spalding (1971)	1.8	$k-\varepsilon$ modelling of round turbulent free jet	
Warhaft and Lumley (1978)	0.6–2.4	Review of heated grid experiments	
Pantano et al. (2003)	1.2–1.6	DNS of reacting planar shear layer	Small Re dependence
Rogers et al. (1986, 1989)	1.6–2	DNS of homogenous turbulent shear flow with different alignments of the mean scalar gradient	Dependence on the alignment

provide estimates of the constant of proportionality between τ_c and τ. Some of these estimates are reported in Table 1.

In conditions of inhomogeneous turbulent mixing (e.g., when the scalar length scale is smaller than the turbulence length scale), τ/τ_c is not constant. For example, Thomson (1996) shows that in the inertial subrange $\tau_c \propto t$, based on similarity arguments, and obtains the coefficient of proportionality as a function of the type of instantaneous release (i.e., point source, infinite line source, and infinite planar source). However, for inhomogeneous mixing Eq. (18) shows that for the IECM model $t_m \neq \tau_c$; while it is still reasonable to assume that $t_m \propto \tau_c$, and therefore that t_m depends on the source type, an exact relationship is not available.

In the limit for $t_m \to 0$, Eq. (17) yields $\sigma_c^2 = \langle\langle c'|\mathbf{u}\rangle^2\rangle_{\mathbf{u}}$. In this case, Sawford (2004) has shown that, for a continuous point or line source in homogeneous turbulence, σ_c^2 obtained by the IECM model is the same as that obtained by a meandering plume model (Gifford, 1959) in which a particular form of the two-point velocity correlation is used in the relative expansion (see also Cohen and Reynolds, 2000, Eqs. (3) and (4)). Following Sawford (2004), this suggests that t_m in the IECM model is associated only to the concentration fluctuations in the frame of reference relative to the centre of mass and, therefore, to the relative dispersion.

In our simulations of releases from localized sources in homogeneous isotropic turbulence, t_m was found to tend to a constant only at large time, i.e., $t > 5\sigma^2/\varepsilon$. Because the experiments reported in this paper were conducted for times smaller than $5\sigma^2/\varepsilon$ we do not define any relationship $t_m \propto \tau$.

3.1. Homogeneous isotropic turbulence

Following Sawford (2004) and Sykes et al. (1984), we assume $t_m = \mu t_r = \mu\sigma_r/\sigma_{ur}$ at short and medium time, where μ is an empirical constant to be evaluated, σ_r is the instantaneous plume spread and $\sigma_{ur} = \langle u_r^2\rangle^{1/2}$is the root mean square (rms) of the relative velocity fluctuations, u_r indicates the difference between a turbulent velocity component and the corresponding velocity component of the instantaneous centre of mass.

σ_{ur} is modelled using the following formulation (Franzese, 2003):

$$\sigma_{ur}^2 = \sigma^2\left(\frac{\sigma_r}{L}\right)^{2/3}, \tag{19}$$

where σ^2 is the variance of the turbulent velocity which is the same in any direction because of isotropy, and $L = (3\sigma^2/2)^{3/2}/\varepsilon$ is a characteristic length scale of the most energetic eddies. Eq. (19) acts as a time-dependent high pass filter that defines σ_{ur}^2 as the fraction of energy contributing to the relative expansion at each stage of the plume growth. This expression is strictly correct only in the inertial sub range. When σ_r equals L all the energy contributes to the expansion, and when σ_r grows larger than L the constraint $\sigma_{ur} = \sigma$ is imposed. This formulation defines $t_m \propto \sigma_r/\sigma_{ur} = (3/2)^{1/2}\tau(\sigma_r/L)^{2/3}$. If σ_r is assumed as the characteristic length scale of the scalar field, this model in the inertial sub range corresponds to the phenomenological model reported by Fox (2003, Eq. (3.15)). The inertial range scaling for t_m was also observed in the experiment by Baldyga et al. (1995). σ_r is parameterised as

$$\sigma_r^2 = \frac{d_r^2}{1 + (d_r^2 - \sigma_0^2)/(\sigma_0^2 + 2\sigma^2 T_L t)}, \tag{20}$$

where

$$d_r^2 = C_r\varepsilon(t_0 + t)^3 \tag{21}$$

with $t_0 = [\sigma_0^2/(C_r\varepsilon)]^{1/3} = t_s/C_r^{1/3}$ is the inertial range formulation for dispersion from a finite source size (Franzese, 2003), C_r is the Richardson–Obukhov constant, σ_0 is the source size and $T_L = 2\sigma^2/C_0\varepsilon$ is the Lagrangian integral time scale. In our simulations, we used $C_r = 0.3$, in agreement with the value obtained by Weil (1994) using the two-particle model of Thomson (1990), and with the value reported in Borgas and Sawford (1994). Parameterisation (20) ensures consistency of σ_r and t_m with the similarity theory of relative dispersion in that $\sigma_r = \sigma_0$ as $t \to 0$; $\sigma_r = d_r$ for $t_s \ll t \ll T_L$; and $\sigma_r = \sqrt{2\sigma^2 T_L t}$ for $t \gg T_L$.

The asymptotic values for t_m are:

$$\begin{aligned} t_m &= \mu_i(3/2)^{1/2}(\sigma_0^2/\varepsilon)^{1/3} \text{ as } t \to 0, \\ t_m &= \mu_i(3/2)^{1/2}C_r^{1/3}\, t \text{ for } t_s \ll t \ll T_L, \\ t_m &= \mu_i\sqrt{2T_L t} \text{ for } d \geqslant L \text{ and } t \gg T_L, \end{aligned} \tag{22}$$

where $i = 1$ for a continuous line source and $i = 2$ for a continuous point source. The coefficients μ_i were empirically estimated from comparisons with the two-particle LS model simulations of Thomson (1990) and depend on the source geometry. For continuous line sources, we find $\mu_1 = (3/2)^{-1/2}$. For continuous point sources a smaller value should be chosen, as indicated by the theoretical analysis of Thomson (1996) and by the semi-empirical analysis of Sawford (2004) and Luhar and Sawford (2005): we used $\mu_2 = 0.8\mu_1$.

3.2. Neutral boundary layer (non-homogeneous non-isotropic turbulence)

The definition of t_m in a neutral boundary layer follows the scheme outlined for homogeneous isotropic turbulence. However, in this case the turbulence statistics are not isotropic and not homogeneous. We define a local mean velocity variance σ^2 by averaging the variances of the three components of velocity, i.e., $\sigma^2 = (\sigma_u^2 + \sigma_v^2 + \sigma_w^2)/3$. A height-dependent t_m is then evaluated in each cell of the discretized domain.

The equation for the relative expansion in the inertial sub range, Eq. (21), is then discretized as

$$d_r^2(t + \Delta t) = d_r^2(t) + 3C_r\varepsilon(t_0 + t)^2\Delta t, \tag{23}$$

where the dissipation $\varepsilon = \varepsilon(z)$ is calculated at the particle position and $d_r^2(0) = \sigma_0^2$. Parameterisation (20) is then used, with the height-dependent quantities σ^2 and T_L calculated at the particle position. The constraint that $\sigma_r^2(t + \Delta t)$ never becomes smaller than $\sigma_r^2(t)$ is also enforced. The turbulence length scale L in Eq. (19) is also local and is computed at each particle position.

Eq. (23) and t_m are calculated using a small sub-ensemble (5000 particles) of the total number of released particles. The sub-ensemble is initially distributed uniformly around the source and is not subject to the procedure of re-sampling and re-initialisation that is used to implement the dynamical grid in the next section. This ensures the necessary continuity of the particle trajectories in the solution of Eq. (23). For each of these particles t_m is calculated at each time step as outlined in Section 3.1. At each vertical level an averaged t_m is calculated by accounting for the contribution of each particle in that cell, and is used in the discretized IECM Eq. (9). Details of the averaging algorithm and numerical integration are given in the next section.

4. Dynamical grid

In general, PDF modelling requires intensive computations because the equations of motion of a sample of all fluid particles, i.e., particles uniformly distributed over the domain, have to be solved. Chemical reactions can be included in closed form if the equations are solved in parallel. The computation is longer the smaller the source size, because the grid should be refined in order to provide details of the field around the source. As a consequence, a large number of particles needs to be simulated in order to have meaningful statistics at each grid point. In this section we describe an efficient numerical procedure based on a time expandable grid, which optimises the calculation. We used 10^5 to 2×10^7 particles, depending on source dimension and geometry, as well as on the number of grid cells (typically 60×60 cells were used). The dynamical grid effectively allows the model to run on standard personal computers for cases of practical interest, such as localized sources in the atmosphere, at least for one and two-dimensional simulations.

The notation $(z_{i+1/2}, y_{j+1/2})$ defines a cell centre, and (z_i, y_j) a node location in the physical space. The grid is used to compute cell-averaged quantities and node-averaged quantities, which are estimators of ensemble-averaged quantities (see Pope, 1985, 2000 and references therein). The cell-averaged quantities are computed using a top hat kernel estimator $\hat{k}_{i+1/2,j+1/2}(z, y)$ centred on the cell centre. Similarly, a cell-averaged quantity at a given height z irrespective of the horizontal crosswind location is computed using a one-dimensional kernel $\hat{k}_{i+1/2}(z)$. Node-averaged quantities are computed using a bi-linear interpolation kernel estimator $\hat{k}_{i,j}(z, y)$centred on the node. Thus the cell-averaged mth moment of concentration at the point (x, y, z) is

$$\langle c^m_{i+1/2,j+1/2}\rangle = \frac{\sum_{n=1}^{N_p}(\hat{k}_{i+1/2,j+1/2}(Z, Y)C^m)_n}{\sum_{n=1}^{N_p}(\hat{k}_{i+1/2,j+1/2}(Z, Y))_n} \tag{24}$$

and similarly for the node-averaged quantities $\langle c^m_{i,j}\rangle$. Here N_p is the total number of particles, (Z,Y) the transverse position of each particle and C is the concentration carried by each particle at the cell location. The cell-averaged t_m is independent of the crosswind location and is calculated from the micromixing time associated with a particle as

$$\langle t_{m_{i+1/2}}\rangle = \frac{\sum_{n=1}^{N_{ps}}(\hat{k}_{i+1/2}(Z)t_m)_n}{\sum_{n=1}^{N_{ps}}(\hat{k}_{i+1/2}(Z))_n}, \tag{25}$$

where N_{ps} is the sub-ensemble of particles used in nonhomogeneous conditions as defined in Section 3.2 above. Average quantities at any point in the domain can be obtained from the node-averaged quantities interpolating from the four surrounding nodes using a bilinear basis function.

A possible solution to ensure an adequate particle density in correspondence of the source is the use of variable spaced structured or unstructured grids coupled with techniques of particle splitting and merging as in the work of Li and Modest (2001). We use a different approach, which is simple and efficient. An initial dynamical grid generated around the source is advected by the mean field and expands around the plume as the plume grows. The expansion involves both the number of cells and their sizes. This procedure saves computational time and memory requirement, and can be implemented as long as the velocity PDF is known. In neutral boundary layer the local mean wind velocity, averaged over the local depth of the plume was taken as advection velocity, which varies with downwind distance from the source. An example of a dynamical grid expanding around a plume in a neutral boundary layer is shown in Fig. 1, where not all nodes are displayed for clarity purposes.

Since the grid extends also to the velocity space, the two-dimensional physical grid corresponds to a four-dimensional phase space grid. The grid is not uniform in the velocity space, where each velocity class includes approximately the same area under the PDF of velocity.

The node-averaged mth moments of concentration conditioned on the velocity classes are calculated as

$$\begin{aligned}&\langle (c_{i,j,l+1/2,m+1/2})^m\rangle \\ &\quad = \langle (c_{i,j}|w_{l+1/2}, v_{m+1/2})^m\rangle \\ &\quad = \frac{\sum_{n=1}^{N_p}(\hat{\hat{k}}_{i,j}(Z,Y)\hat{k}_{l+1/2,m+1/2}(W,V)C^m)_n}{\sum_{n=1}^{N_p}(\hat{\hat{k}}_{i,j}(Z,Y)\hat{k}_{l+1/2,m+1/2}(W,V))_n}.\end{aligned} \tag{26}$$

Therefore, the calculation proceeds according to the following scheme:

(1) First, a small uniform grid is created around the source. The grid is large enough to ensure that the Gaussian concentration distribution centred at the source is negligible at the boundary cells. The initial particle velocity is extracted from the local velocity PDF.
(2) The updated particle position and velocity are calculated.
(3) Boundary conditions are checked. The physical boundaries are treated as perfectly reflecting barriers for particle position, velocity and concentration. The computational boundaries are treated as absorbing barriers for concentration. For non-Gaussian turbulence a different procedure for the reflected velocity should be used (Cassiani et al., 2005).
(4) Cell-averaged and node-averaged quantities are computed and stored.
(5) $\langle c|\mathbf{X},\mathbf{U}\rangle$ is obtained interpolating $\langle c_{i,j}|w_{l+1/2}, v_{m+1/2}\rangle$ and is used in the following discretized IECM equation,

$$C(t+\Delta t) = C(t) - \left\{1 - \exp\left(-\frac{1}{t_m}\Delta t\right)\right\}(C(t) - \langle c|\mathbf{X},\mathbf{U}\rangle), \tag{27}$$

where $C(t)$is the particle concentration.
(6) A grid expansion condition is checked. The condition is based on the ratio of minimum to maximum cell-averaged mean concentration in each physical direction. The amount of the fractional expansion in each direction is determined from the rate of growth of the mean plume spreads σ_y and σ_z at each time. The expansion proceeds asymmetrically if the computational domain reaches a physical boundary.
(7) After the expansion of the computational domain, N_E particles are sampled from the total number of

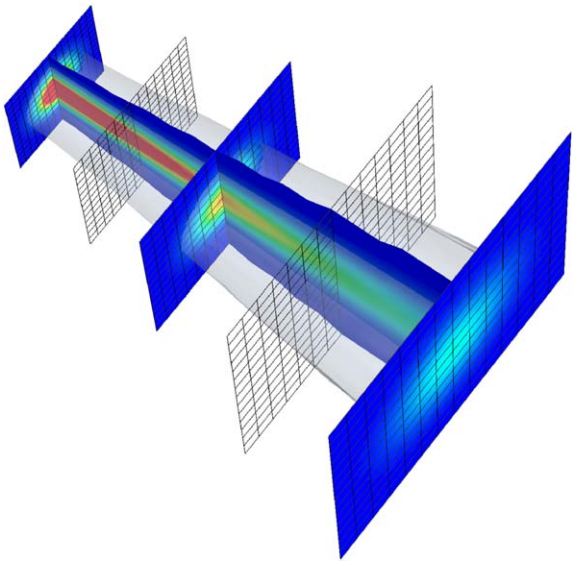

Fig. 1. Example of a dynamical grid expansion around a plume in a neutral boundary layer.

particle N_P and are uniformly positioned in the fraction of computational domain just added with zero concentration and a velocity extracted from the local PDF. N_E is calculated to ensure that the total number of particles after expansion remains uniformly distributed in the computational domain.

(8) Finally, each grid cell is also expanded ensuring the conservation of the number of particles in each cell. A maximum cell size is imposed to ensure that the grid does not artificially spread mean concentration through the cell expansion process. In this case, the number of cells is increased to not exceed the maximum cell size.

The integration time step in the model equations was always one or two orders of magnitude smaller than the minimum among: (i) the time scale defined by size of the domain and rms velocity; (ii) the turbulence Lagrangian time scale; and (iii) the micromixing time scale.

5. Dispersion simulations in homogeneous isotropic turbulence. Comparison with two-particle LSM simulations and experiments

The intensity of concentration fluctuations $\sigma_c/\langle c\rangle$ along the centreline of the plume in homogeneous isotropic turbulence was simulated for releases from a point source and from an infinite line source. Fig. 2 shows the simulation results (continuous lines) for line sources with source sizes ranging from $\sigma_0 = 10^{-3}\sigma^3/\varepsilon$ to $\sigma_0 = 0.2\sigma^3/\varepsilon$, the symbols are the corresponding predictions of Thomson's (1990) two-particles model. Maximum values of $\sigma_c/\langle c\rangle$ and locations of the maxima, which are very sensitive to source size, are reproduced

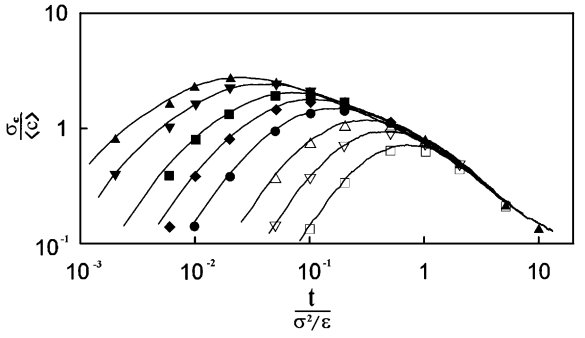

Fig. 2. Variation of the intensity of concentration fluctuations along the centreline of the plume with dimensionless time for an infinite continuous line source as predicted by our model (lines) and by Thomson (1990) two-particle model (symbols). The lines correspond to the following source sizes σ_0, from left to right: $0.001\sigma^3/\varepsilon$, $0.002\sigma^3/\varepsilon$, $0.005\sigma^3/\varepsilon$, $0.01\sigma^3/\varepsilon$, $0.02\sigma^3/\varepsilon$, $0.05\sigma^3/\varepsilon$, $0.1\sigma^3/\varepsilon$, $0.2\sigma^3/\varepsilon$.

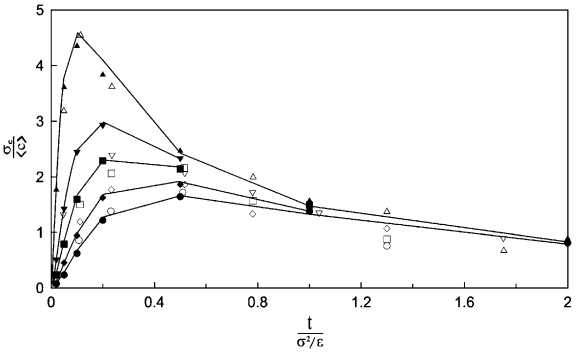

Fig. 3. Variation of the intensity of concentration fluctuations along the centreline of the plume with dimensionless time for a continuous point source as predicted by our PDF-IECM model (lines) and by Thomson (1990) two-particle model (solid symbols), along with the observations from Fackrell and Robins (1982a) experiments (open symbols). Different symbols refer to different source sizes: ▲ $\sigma_0 = 7.41 \times 10^{-3}\sigma^3/\varepsilon$, ▼ $\sigma_0 = 2.22 \times 10^{-2}\sigma^3/\varepsilon$, ■ $\sigma_0 = 3.7 \times 10^{-2}\sigma^3/\varepsilon$, ◆ $\sigma_0 = 6.17 \times 10^{-2}\sigma^3/\varepsilon$, ● $\sigma_0 = 8.64 \times 10^{-2}\sigma^3/\varepsilon$.

with minimal error. The time decay of $\sigma_c/\langle c\rangle$ is also satisfactorily captured although small differences cannot be appreciated on a logarithmic scale.

The good agreement between our model and Thomson's model is also apparent in Fig. 3, which shows $\sigma_c/\langle c\rangle$ for a point source, as a function of time on a linear scale. The lines in Fig. 3 represent the results of the PDF-IECM model, the solid symbols the results of Thomson's (1990) model. There are only minor differences between the predictions of the two models. Fig. 3 also shows the measurements of the wind tunnel experiment of Fackrell and Robins (1982a) as originally reported in Thomson (1990). The effects of anisotropy and non-homogeneity, which are present in the experiments, are neglected in these simulations. The initial scalar distribution in the simulations was a Gaussian with standard deviation σ_0 equal to the physical source diameter. This choice may have a certain degree of arbitrariness (see also the discussion in Fackrell and Robins, 1982b). For instance, a different but still reasonable choice is to assume the initial spread equal to the radius instead of the diameter of the source (Sykes et al., 1984). Another approximation in the comparison with the experiment was introduced because the simulated $\sigma_c/\langle c\rangle$ is calculated along the plume centreline, whereas the observed $\sigma_c/\langle c\rangle$ was calculated as the ratio of $\max(\sigma_c)$ to $\max(\langle c\rangle)$ which were not necessarily measured at the same crosswind position. Because of the above uncertainties, the good agreement between experiment and simulations may be regarded as partially fortuitous.

In the next section, anisotropy and non-homogeneity in Fackrell and Robins (1982a) experiment will be

accounted for in the simulations, and slightly different source size definitions are found to provide more accurate results.

6. Dispersion simulations in neutral boundary layer—comparisons with experiments

Fackrell and Robins (1982a) wind tunnel experiments were designed mainly to examine the effects of source sizes on concentration fluctuations from ground level and elevated releases. The boundary layer generated in the wind tunnel corresponds to an atmospheric neutral boundary layer.

The observed velocity variance and dissipation profiles were fit by analytical curves and used as an input to our model. The mean wind averaged over the local depth of the plume is used as advection velocity. Shear effects were neglected. In general, the effects of neglecting the shear are reduced as the distance from the source increases because the mixing processes reduce the mean gradients of concentration. For elevated releases, crosswind and vertical meandering are the main source of concentration fluctuations close to the source. Therefore, this approximation is expected to be relatively unimportant for elevated releases because the shear close to the source is weaker and the plume nears the ground at a distance from the source. For ground level releases, neglecting the shear should cause an underestimate of concentration fluctuations close to the source. The approximation was not found to introduce significant errors in any of the investigated cases. The Kolmogorov constant for the Lagrangian velocity structure function $C_0 = 5$ produced a good agreement between simulated and observed mean concentration fields. The simulated initial spread σ_0 was related to the diameter D_o of the physical source as $\sigma_0^2 = (2/3)D_o^2$. This value was found to give a good agreement in the simulation of the initial growth of the fluctuation intensity for all sources while, in general, the source sizes does not significantly influence the mean field. All results and observations presented were obtained at the plume centreline $y = 0$.

Fig. 4 a and b report vertical profiles of $\langle c \rangle$ and σ_c^2, respectively, scaled by their maximum values along each profile, at several distances from the source. The release elevation was $0.19h$, where h is the boundary layer height. The lines refer to our simulations, the open symbols to the experiments; the source diameter in the experiments is 8.5 mm, which corresponds to a simulated initial spread $\sigma_0 \approx 7$ mm. Fig. 4 shows that the simulated maximum $\langle c \rangle$ and maximum σ_c^2 occur at different elevations, especially far from the source, in very good agreement with the experiments. In particular, the good fit near the ground indicates that the definition of t_m in

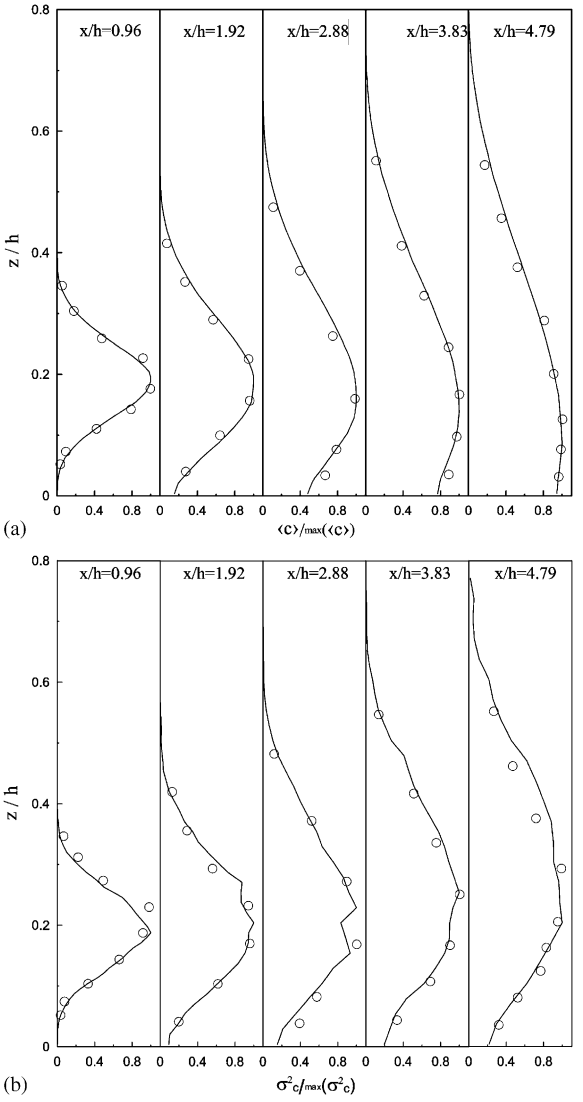

Fig. 4. Vertical profiles of mean concentration $\langle c \rangle$ scaled with the maximum mean concentration $\max(\langle c \rangle)$ (a), and vertical profiles of mean square concentration σ_c^2 scaled with the maximum concentration variance $\max(\sigma_c^2)$ (b), at five downwind distances for an elevated source at 0.19 h and a source diameter of 8.5 mm.

inhomogeneous turbulence outlined in Section 3.2 correctly captures the physics of the dispersion process, and that the approximation introduced neglecting the shear effects on the mean wind is acceptable.

Fig. 5 shows the variation with distance of the maximum σ_c scaled with the maximum $\langle c \rangle$ for elevated and ground level releases. The elevated release experiments were conducted for five different sources with diameter ranging between 3 and 35 mm.The observations for the elevated release are reported as open

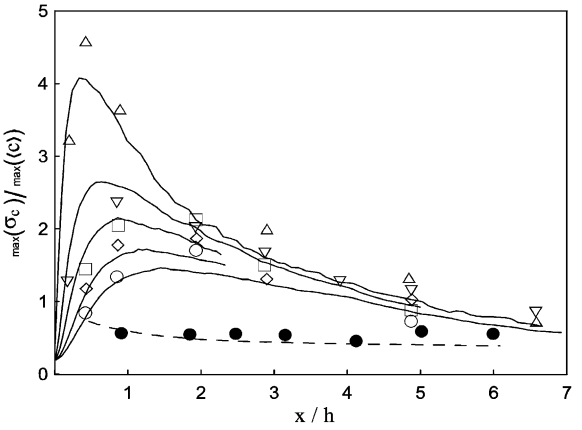

Fig. 5. Measured and modelled concentration fluctuation intensity defined as maximum root mean square concentration $\max(\sigma_c)$ scaled with the maximum mean concentration $\max(\langle c\rangle)$ at each downwind distance. The open symbols are Fackrell and Robins (1982a) experimental data for elevated releases with source diameter: ○ 35 mm, ◇ 25 mm, □ 15 mm, ▽ 8.5 mm and △ 3 mm; the solid lines are our simulations. The solid circles are the experimental results for the ground level release with a source diameter of 15 mm, the dashed line is our corresponding simulation.

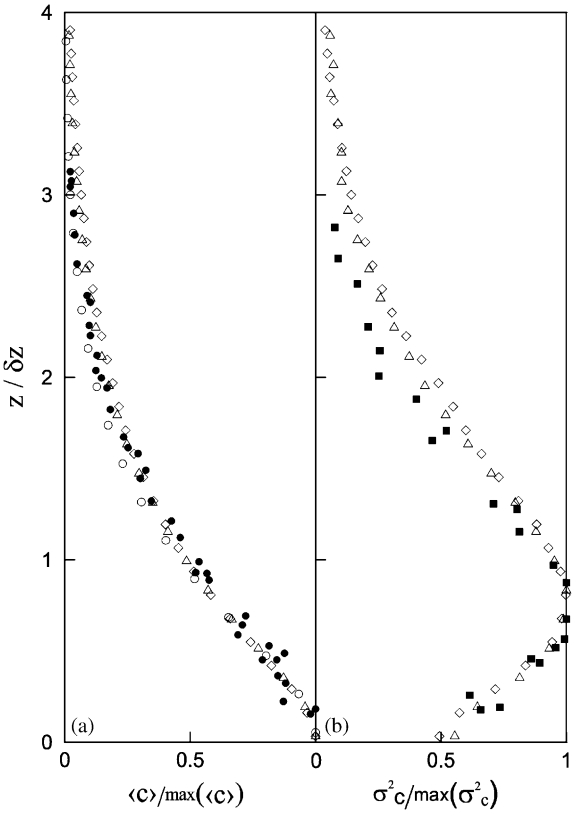

Fig. 6. (a) Measured and modelled mean concentration scaled over the maximum value at each downwind distance. Solid circles refer to the experimental observations of Fackrell and Robins (1982a) in the downwind range $1.67 < x/h < 5.92$. Open symbols refer to model simulations: ○ $x/h = 1.67$; △ $x/h = 2.5$; ◇ $x/h = 5$. (b) Measured and modelled concentration variance scaled over the maximum value at each downwind distance. Solid squares refer to experimental observations of Fackrell and Robins (1982a) in the downwind range $3.33 < x/h < 5.92$. Open symbols as already reported in (a). The vertical coordinate is scaled with δz, which is defined as the vertical position of one half the maximum value of the mean concentration.

symbols, our simulations are plotted as continuous lines. The solid circles are the observations for a ground level source with a diameter of 15 mm; the dashed line is the corresponding simulation.

Fig. 6 a and b show the observed and simulated vertical profiles of $\langle c\rangle$ and σ_c^2, respectively, for the ground level release with a source diameter of 15 mm for all downwind distances. $\langle c\rangle$ and σ_c^2 are scaled with their respective maxima at each downwind distance. The elevation is scaled with the quantity δz, which is defined as the elevation where $\langle c\rangle$ is one half of its maximum along the vertical profile. This type of scaling emphasizes a self-similar behaviour with distance from the source and allows the representation of the data at different downwind distances in the same plot, as suggested by Fackrell and Robins (1982a). The solid symbols in Fig. 6 refer to experimental results, the open symbols to simulations. All measurements reported in Fig. 6a were taken in the range $1.67 < x/h < 5.92$; all measurements in Fig. 6b were in the range $3.33 < x/h < 5.92$. The open symbols in both Fig. 6 a and b are simulation data points at the three downwind distances $x/h = 1.67$, 2.5 and 5.

Fig. 7 shows a comparison of modelled and measured PDF of concentration $f(c)$ at the downwind distance $x/h = 4.79$, at three different elevations. The observations indicate that $f(c)$ has a clipped-gaussian like form near the ground, and tends to an exponential like form far from the ground. The simulation reproduces quite well the observed $f(c)$ at the elevated sampling location $z = 0.38\,h$, but the agreement worsens at lower elevations, where the experiments indicate that $f(c)$ relaxes towards a clipped Gaussian and the simulation essentially underestimates the probability of concentration lower than the mean. This is possibly due to the sensitivity of the evolution of the shape of $f(c)$ generated by the IECM model to the initial distribution of concentration. In a statistically homogenous scalar field the evolution of $f(c)$ towards the correct asymptotic shape can be obtained in the presence of a constant mean scalar gradient. In general the stronger the mean concentration gradient the smaller t_m and the faster the relaxation towards the asymptotic PDF. This suggests that the IECM model performs better for

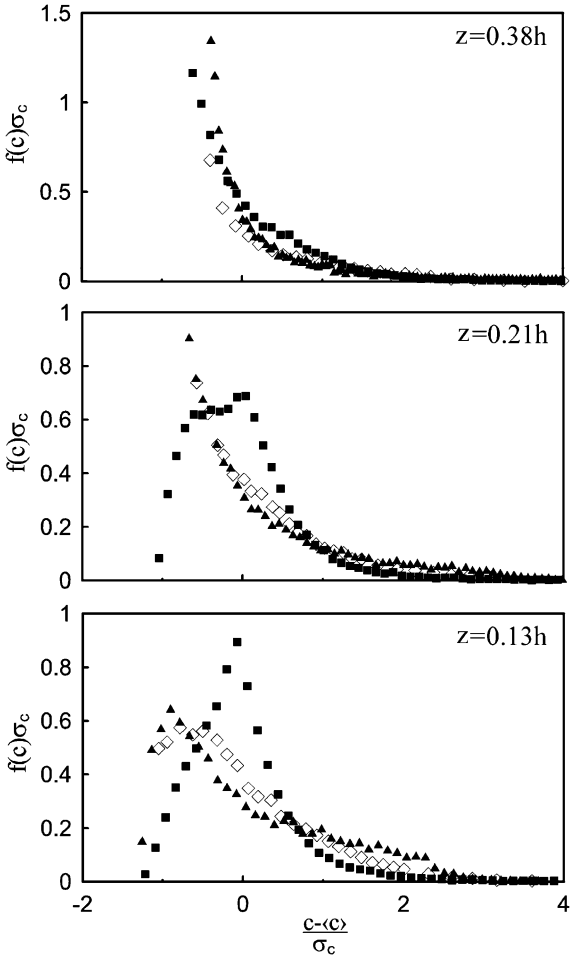

Fig. 7. Probability density function of concentration $f(c)$ at $x/h = 4.79$ and $y/h = 0$ at different elevation from the ground: ■, simulations for an elevated ($z/h = 0.19$) release; ▲ simulations for a ground level release; ◇ Fackrell and Robins (1982a) experiment for an elevated ($z/h = 0.19$) release.

ground level releases where there are stronger gradients of mean concentration and t_m remains relatively small for longer time. Since the observed $f(c)$ at the measurement distance is expected to be quite insensitive to the source elevation, the simulation of a ground level release in Fig. 7 matches the observations better than the elevated release.

7. Conclusion

The PDF modelling is commonly applied to problems of combustion turbulence and chemical engineering as an effective technique to calculate the one point PDF of passive and reactive scalars dispersing in turbulent flow. We have applied this technique to the prediction of the concentration PDF for releases from small sources in the atmosphere under neutral conditions.

Our modelling is based on the micromixing modelling approach used in the chemical engineering framework coupled with the Lagrangian stochastic modelling used in atmospheric dispersion studies.

The model is currently limited to two-dimensional simulations but it can readily be applied to three-dimensional releases neglecting the along wind dispersion and shear effects. The results were in overall good agreement with Lagrangian two-particle model simulations of releases from point and line sources in homogeneous isotropic turbulence and with the wind tunnel experiments of Fackrell and Robins (1982a) for ground level and elevated releases from various source sizes in the non-homogeneous turbulence of a neutral boundary layer. The observed mean and rms concentration in the neutral boundary layer are reproduced with a negligible error. The simulation of the full concentration PDF $f(c)$ gives a satisfactory qualitative and quantitative agreement, although discrepancies arise in the comparison with $f(c)$ near ground. These discrepancies can be attributed to the simple form of the IECM model and are expected to improve for ground level releases.

More sophisticated formulations for the micromixing model including a stochastic forcing and a more elaborate definition of the term φ in Eq. (6) can be formulated as reported in, e.g., Valino and Dopazo (1991), Heinz (2003), and Fox (2003). These formulations ensure the relaxation of $f(c)$ to a Gaussian form at large time even for an initial homogeneous concentration field. However, the implementation of a stochastic forcing is not straightforward because of the boundedness of the scalar field. These models are less efficient than a deterministic IECM model, and the expected gain in accuracy may not justify their use in most applications, nevertheless testing the performances and computational requirements of alternate formulations in atmospheric flow is an interesting task for future studies.

The model developed in this paper was applied to simulations of passive scalars. However, because the particles are tracked in parallel it can account for chemical reactions in a direct way with no closure assumptions. The natural extension of this study includes the complete simulation of atmospheric releases of reactive substances including chemical reactions.

Acknowledgements

We acknowledge Dr Brian Sawford for helpful discussions in the early stage of this work and for sending us the preprints of his works. We also acknowledge Alexandre Radicchi for helpful comments.

References

Baldyga, J., Bourne, R.J., Dubuis, B., Etchells, A.W., Gholap, R.V., Zimmerman, B., 1995. Jet reactor scale-up for mixing-controlled reaction. Transactions of the Institution of Chemical Engineering 73, 497–502.

Bisignanesi, V., Giostra, U., Cassiani, M., 2002. Modelli a PDF per lo studio della dispersione di inquinanti reattivi. Thesis of Laurea (in Italian). University of Urbino, Italy.

Borgas, M.S., Sawford, B.L., 1994. A family of stochastic model for two-particle dispersion in isotropic homogeneous stationary turbulence. Journal of Fluid Mechanics 279, 69–99.

Cassiani, M., Giostra, U., 2002. A simple and fast model to compute concentration moments in a convective boundary layer. Atmospheric Environment 36, 4717–4724.

Cassiani, M., Franzese, P., Giostra, U., 2005. A PDF micromixing model of dispersion for atmospheric flow. Part II: application to convective boundary layer. Atmospheric Environment, doi:10.1016/j.atmosenv.2004.11.019

Chatwin, P.C., 2004. Singular PDFs of a dispersing scalar in turbulence. Flow Turbulence and Combustion 72, 273–285.

Cohen, J.E., Reynolds, A.M., 2000. Parameterisation of the two-point velocity correlation function in a two-particle Lagrangian stochastic model and its effect on the prediction of concentration variance due to a line source. Journal of Applied Meterology 39, 1762–1769.

Dopazo, C., 1976. A probabilistic approach to the turbulent mixing of reacting scalars. American Meteorological Society Third Symposium on Atmospheric Turbulence, Diffusion and Air Quality, 19–22 October, Raylegh, North Carolina.

Dopazo, C., O'Brien, E.E., 1974. An approach to the auto ignition of a turbulent mixture. Acta Astronautica 1, 1239–1266.

Dopazo, C., Valino, L., Fuego, F., 1997. Statistical description of the turbulent mixing of scalar fields. International Journal of Modern Physics B 11 (25).

Eswaran, V., Pope, S.B., 1988. Direct numerical simulation of the turbulent mixing of a passive scalar. Physics of Fluids, 31, 506.

Fackrell, J.E., Robins, A.G., 1982a. Concentration fluctuations and fluxes in plumes from point sources in a turbulent boundary layer. Journal of Fluid Mechanics 117, 1–26.

Fackrell, J.E., Robins, A.G., 1982b. The effect of source size on concentration fluctuations in plumes. Bound. Layer Meteorology 22, 335–350.

Fox, R.O., 1996. On velocity conditioned scalar mixing in homogeneous turbulence. Physics of Fluids, 8, 2678−2691.

Fox, R.O., 2003. Computational Models for Turbulent Reacting Flows. Cambridge University Press, Cambridge 419 pp.

Franzese, P., 2003. Lagrangian stochastic modelling of a fluctuating plume in the convective boundary layer. Atmospheric Environment 37, 1691–1701.

Gardiner, C.W., 1983. Handbook of Stochastic Methods for Physics Chemistry and the Natural Sciences. Springer, New York, 442 pp.

Georgopoulis, P.G., Seinfeld, J.H., 1986. Mathematical modelling of turbulent reacting plumes-I. General theory and model formulation. Atmospheric Environment 20 (9), 1791–1807.

Gifford, F.A., 1959. Statistical properties of a fluctuating plume dispersion model. Advances in Geophysics 6, 117–137.

Gonzalez, M., 1997. Analysis of the effect of microscale turbulence on atmospheric chemical reactions by means of the PDF approach. Atmospheric Environment 31, 575–586.

Griffith, R.F., Megson, L.C., 1984. The effect of uncertainties in human toxic response on hazard range estimation for ammonia and chlorine. Atmospheric Environment 18, 1195–1206.

Heinz, S., 2003. Statistical Mechanics of Turbulent Flows. Springer, Berlin, Heidelberg, Germany, 214 pp.

Hilderman, T.L., Hrudey, S.E., Wilson, D.J., 1999. A model for effective toxic load from fluctuating gas concentrations. Journal of Hazardous Materials A, 64, 115–134.

Kernstein, A.L., 1991. Linear-eddy modelling of turbulent transport. Part. 6. Microstructure of diffusive scalar mixing fields. Journal of Fluid Mechanics 231, 361–394.

Li, D.J., Bilger, R.W., 1996. The diffusion of conserved and reactive scalars behind line sources in homogeneous turbulence. Journal of Fluid Mechanics 318, 339–372.

Li, G., Modest, M.F., 2001. An effective particle tracking scheme on structured/unstructured grids in hybrid finite volume/PDF Monte Carlo methods. Journal of Computer Physics 173, 187–201.

Luhar, A.K., Hibberd, M.F., Borgas, M.S., 2000. A Skewed meandering plume model for concentration statistics in the convective boundary layer. Atmospheric Environment 34, 3599–3616.

Luhar, A.K., Sawford, B.L., 2005. Micromixing modelling of concentration fluctuations in inhomogeneous turbulence in the convective boundary layer. Bound. Layer Meteorol. 114, 1–30.

Monin, A.S., Yaglom, A.M., 1975. Statistical Fluid Mechanics, vol. 2. MIT Press, Cambridge, MA, 874 pp.

O'Brien, E.E., Myers, R.E., Benkovitz, C.M., 1976. Chemically reactive turbulent plumes. Proceeding American Meteorological Society Third Symposium on Atmospheric Turbulence, Diffusion and Air Quality, 19–22 October, Raylegh, North Carolina, pp. 155–159.

Overholt, M.R., Pope, S.B., 1996. Direct numerical simulation of a passive scalar with imposed mean gradient in isotropic turbulence. Physics of Fluids, 8 (11), 3128–3148.

Pantano, C., Sarkar, S., Williams, F.A., 2003. Mixing of a conserved scalar in a turbulent reacting shear layer. Journal of Fluid Mechanics 481, 291–328.

Pope, S.B., 1985. PDF methods for turbulent reactive flows. Progress in Energy Combustion Science 11, 119–192.

Pope, S.B., 1994. Lagrangian PDF methods for turbulent flows. Annual Revlaist Fluid Mechanics 26, 23–63.

Pope, S.B., 1998. The vanishing effect of molecular diffusivity on turbulent dispersion: implications for turbulent mixing and the scalar flux. Journal of Fluid Mechanics 359, 299–312.

Pope, S.B., 2000. Turbulent Flows. Cambridge University Press, Cambridge, 806 pp.

Rogers, M.M., Moin, P., Reynolds, W.C., 1986. The structure and modelling of the hydrodynamic and passive scalar fields in homogenous turbulent shear flow. Department of mechanical engineering report No. TF-25, Stanford University.

Rogers, M.M., Mansour, N.N., Reynolds, W.C., 1989. An algebraic model for turbulent flux of a passive scalar. Journal of Fluid Mechanics 204, 77.

Sawford, B.L., 2004. Micro-mixing modelling of scalar fluctuations for plumes in homogeneous turbulence. Flow Turbulence and Combustion 72, 133–160.

Spalding, D., 1971. Concentration fluctuations in a round turbulent free jet. Chemical Engineering Science 26, 95–107.

Subramaniam, S., Pope, S.B., 1998. A mixing model for turbulent reactive flows based on Euclidean minimum spanning trees. Combustion and Flame, 115, 487–514.

Sykes, R.I., Lewellen, W.S., Parker, S.F., 1984. A turbulent transport model for concentration fluctuation and fluxes. Jurnal of Fluid Mechanics 139, 193–218.

Tavoularis, S., Corrsin, S., 1981. Experiments in nearly homogeneous turbulent shear flow with a uniform mean temperature gradient. Part I. Jurnal of Fluid Mechanics 104, 311–347.

Thomson, D.J., 1987. Criteria for the selection of the stochastic models of particle trajectories in turbulent flows. Jurnal of Fluid Mechanics 180, 529−556.

Thomson, D.J., 1990. A stochastic model for the motion of particle pairs in isotropic high-Reynolds-number turbulence, and its application to the problem of concentration variance. Jurnal of Fluid Mechanics 210, 113–153.

Thomson, D.J., 1996. The second-order moment structure of dispersing plumes and puffs. Jurnal of Fluid. Mechanics 320, 305.

Valino, L., Dopazo, C., 1991. A binomial Langevin model for turbulent mixing. Physics of Fluids A, 3 (12), 3034–3037.

Villermaux, J., Devillon, J.C., 1972. In: Proceeding of the Second International Symposium On Chemical Reaction Engineering, New York, Elsevier.

Wandel, P.A., Smith, N.S.A., Klimenko, A.Y., 2003. Verification of Markov hypothesis for conserved scalar process: Validation of conditional moment closure for turbulent combustion. ANZIAM Journal 44 (E), C802-C819.

Warhaft, Z., 2000. Passive scalars in turbulent flows. Annual Revier of Fluid Mechanics 26, 211–254.

Warhaft, Z., Lumley, J.L., 1978. An experimental study of the decay of temperature fluctuation in grid-generated turbulence. Jurnal of Fluid Mechanics 88, 659.

Weil, J.C., 1994. A hybrid Lagrangian dispersion model for elevated source in the convective boundary layer. Atmospheric Environment 28, 3433–3448.

Wilson, D.J., 1995. Concentration Fluctuations and Averaging Time in Vapor Clouds. Center for Chemical Process Safety. American Institute of Chemical Engineers, New York, 181 p.